Supporting Information

Modulation of CO_2 Adsorption in Novel Pillar-layered MOFs Based on Carboxylate-pyrazole Flexible Linker

Andres Lancheros[1,2,3], Subhadip Goswami[3], Mohammad Rasel Mian[3], Xuan Zhang[3], Ximena Zarate[4], Eduardo Schott[1,2]*, Omar K. Farha,[3] Joseph T. Hupp[3]*

[1] Departamento de Química Inorgánica, Facultad de Química y Farmacia, Centro de Energía UC, Centro de Investigación en Nanotecnología y Materiales Avanzados CIEN-UC, Pontificia Universidad Católica de Chile, Avenida Vicuña Mackenna 4860, Santiago, Chile
[2]ANID -Millennium Science Initiative Program- Millennium Nuclei on Catalytic Process Towards Sustainable Chemistry (CSC), Chile
[3] Department of Chemistry and International Institute for Nanotechnology, Northwestern University, 2145 Sheridan Road, Evanston, Illinois 60208, United States
[4] Instituto de Ciencias Químicas Aplicadas, Theoretical and Computational Chemistry Center, Facultad de Ingeniería, Universidad Autónoma de Chile, Av. Pedro de Valdivia 425, Santiago, Chile.

Synthesis and Characterization of H_2L

The linker (H_2L) was synthesized in two steps according to previous reports[1,2]

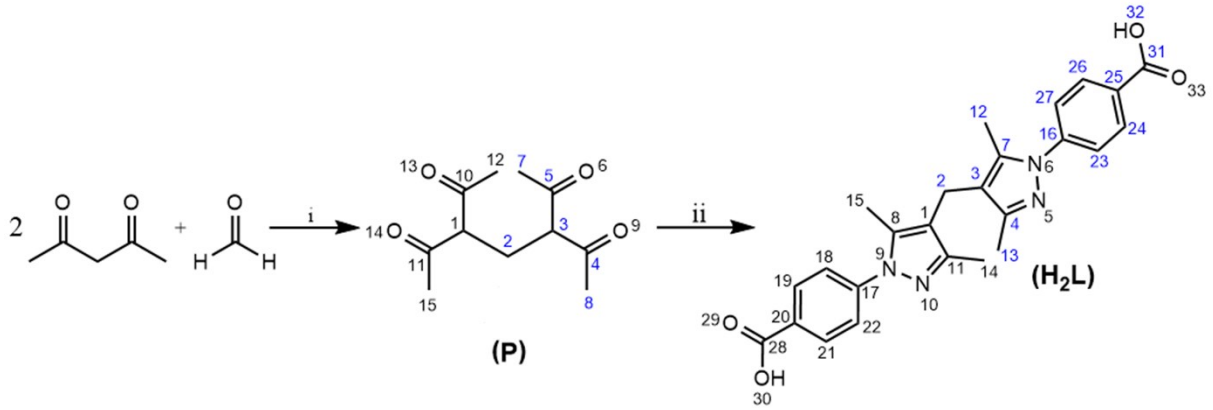

i) 5 days. **ii**) AcOH, EtOAc, 4-hydrazinobenzoic acid, 24 h, reflux
Scheme 1. Synthesis of H_2L

Step 1. Synthesis of 3,5-diacetylheptane-2,6-dione (P).[2]

In a round-bottomed flask of 100 mL, a mixture of acetylacetone (20.00 mL, 0.200 mol) and formaldehyde (37% aqueous solution, 13.50 mL, 0.490 mol) was stirred at 1000 rpm for 5 days. When completed, two phases were formed, on the top a light-yellow aqueous layer (~10 mL) and on the bottom gold-colored organic layer (~40 mL). The mixture was separated using a separating funnel. The organic layer was dried over $MgSO_4$, an equal volume of diethyl ether was added and then it was cooled in an ice-ethanol bath to produce white solid (P) (**Scheme 1**). The product was filtered and washed three times with ethyl ether. Finally, it was dried in a vacuum oven at 60 °C for 12 hours.

Yield: 30%. **^{1}H NMR (**400 MHz, $CDCl_3$, 298K): δ/ppm= 3.63 (t, J_{HH}=6.21 Hz, 2H, H_3), 2.25 (t, J_{HH}=6,10 Hz, 2H, H_2), 2.18 (s, 12H, $H_{7,8}$). **^{13}C NMR {^{1}H}** (100 MHz, $CDCl_3$, 298K): δ/ppm=

203.69 ($C_{4,5}$), 64.96 (C_3), 29.69 (C_7,C_8), 25.04 (C_2).**DEPT-135** (100 MHz, $CDCl_3$, 298 K): δ/ppm = 64.84 (C_3), 29.57 ($C_{7,8}$), 24.92 (C_2). **^{1}H,^{13}C-HSQC** (400 MHz/100 MHz, $CDCl_3$, 298 K): δ(^{1}H)/δ(^{13}C) = 3.63/64.96 (H_3/C_3), 2.25/25.01 (H_2/C_2), 2.19/29.72 ($H_{7,8}$/$C_{7,8}$). **^{1}H,^{13}C-HMBC** (400 MHz/100 MHz, $CDCl_3$, 298 K): δ(^{1}H)/δ(^{13}C)= 2.18/203.69 ($H_{7,8}$/$C_{4,5}$). **FT-IR (KBr):** ν/cm^{-1}= 3402.43 (w), 1689.64 (m), 1427.32 (w), 1365.60 (w), 1319.31 (w), 1149.57 (m), 1080.14 (w), 1041.56 (w), 956.59 (s), 879.54 (w), 810.10 (s), 732.95 (m), 648.08 (m), 594.08 (s), 555.50 (s), 493.78 (s), 493.78 (s), 362.02 (m), 324.04 (m) **HRMS(HESI):** m/z [M+H]$^+$ calculated for $C_{11}H_{16}O_4$ (213.11), found 213.1121. **UV** (nm): 291.

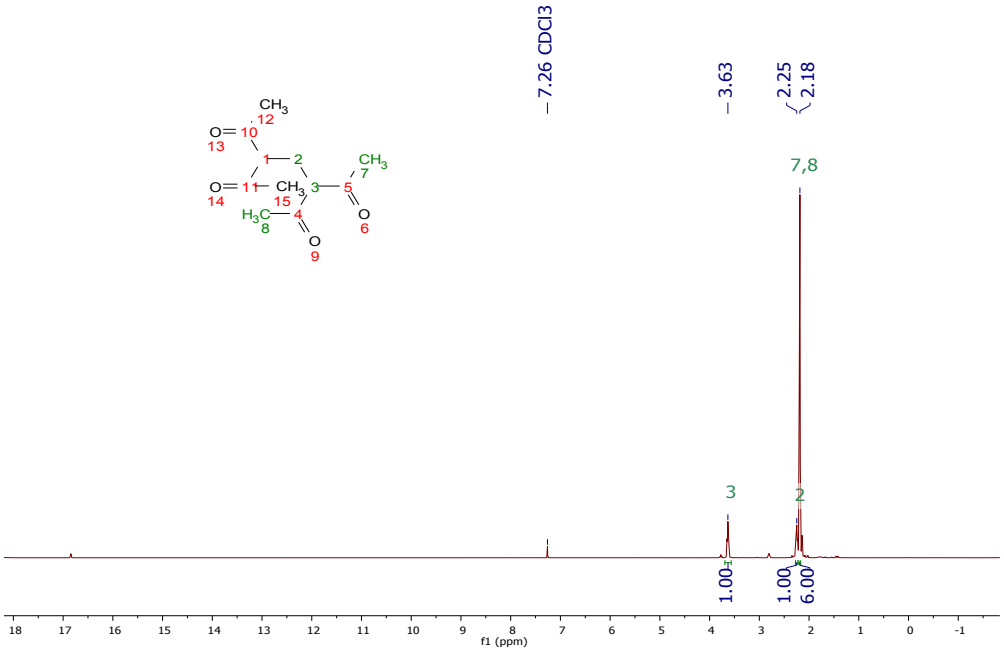

Figure S1. 400 MHz ^{1}H NMR spectrum of P in $CDCl_3$

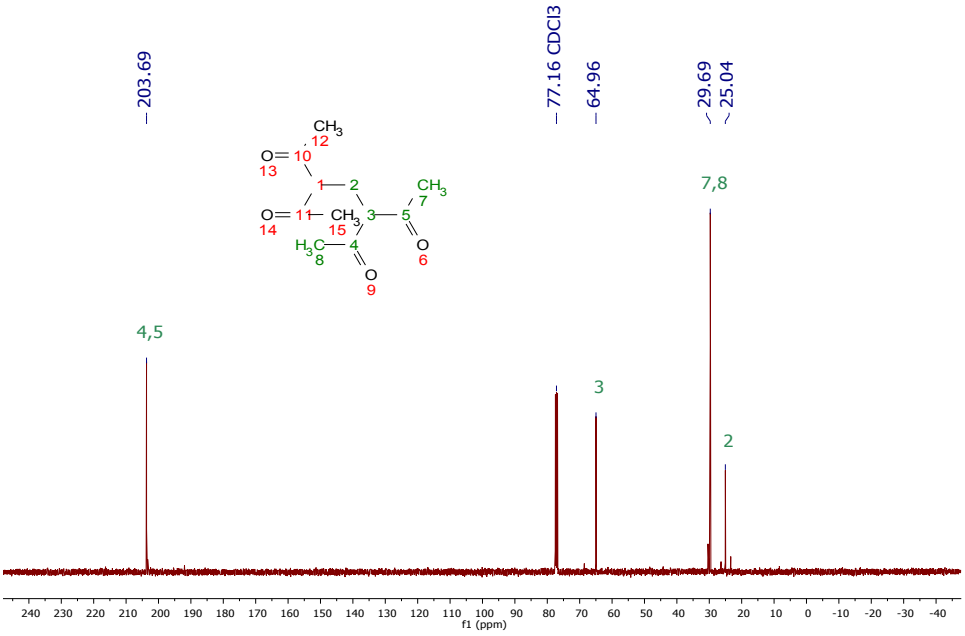

Figure S2. 400 MHz ^{13}C NMR spectrum of P in $CDCl_3$

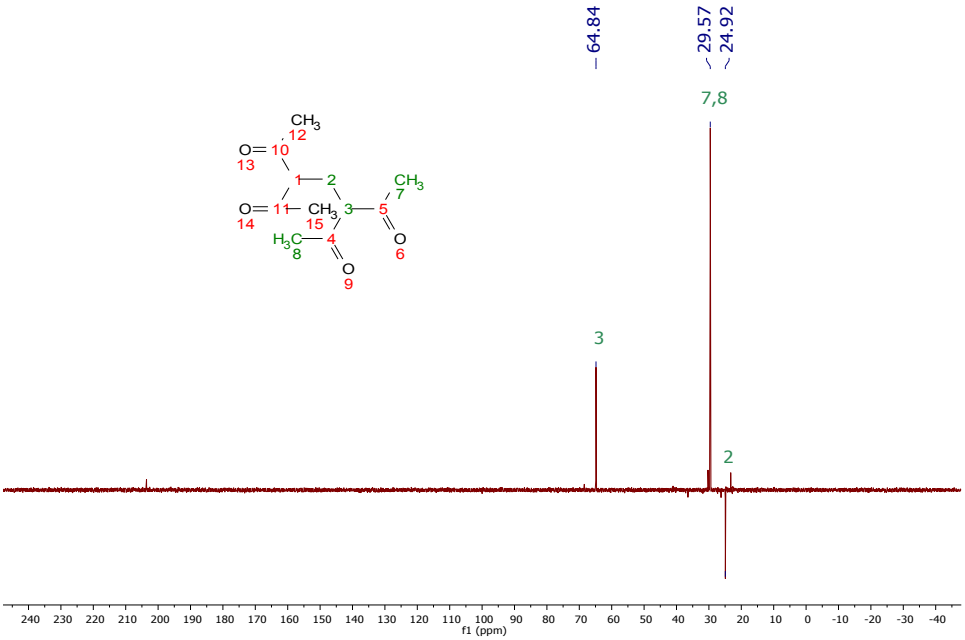

Figure S3. 400 MHz DEPT-135 NMR spectrum of P in $CDCl_3$

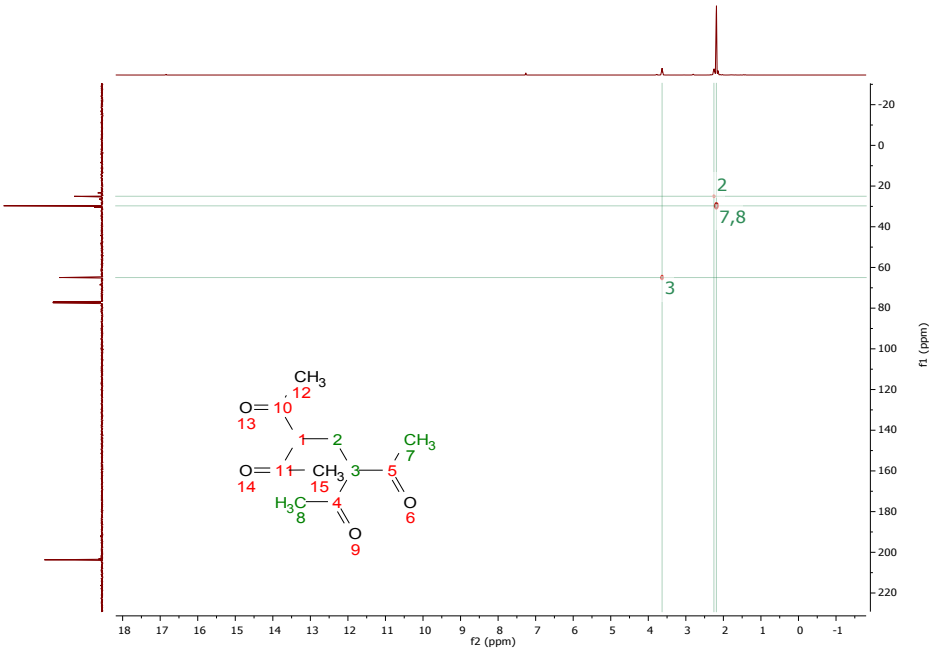

Figure S4. 400 MHz HSQC NMR spectrum of P in $CDCl_3$

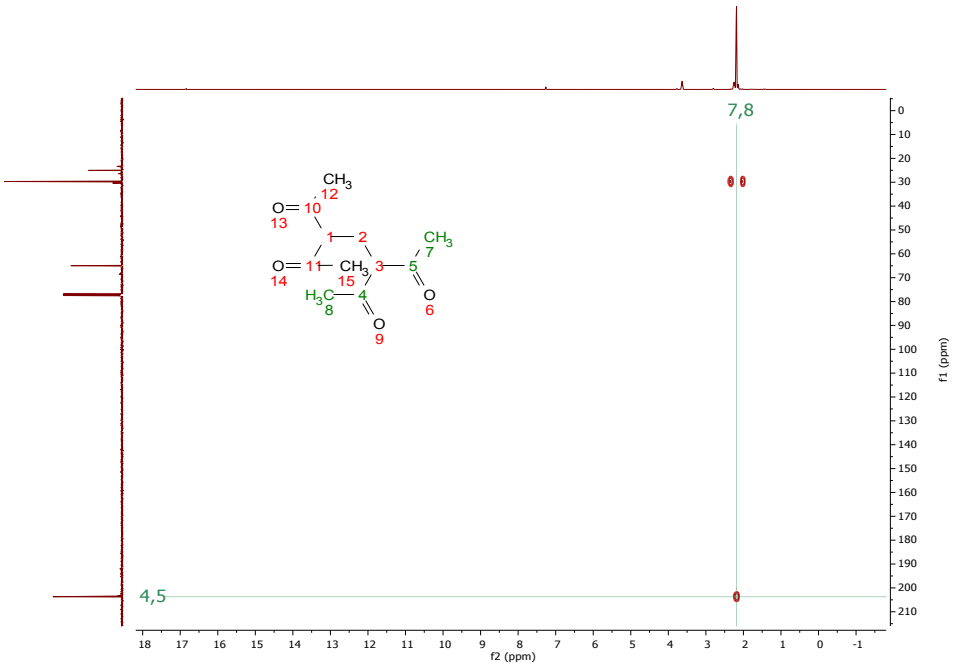

Figure S5. 400 MHz HMBC NMR spectrum of P in $CDCl_3$

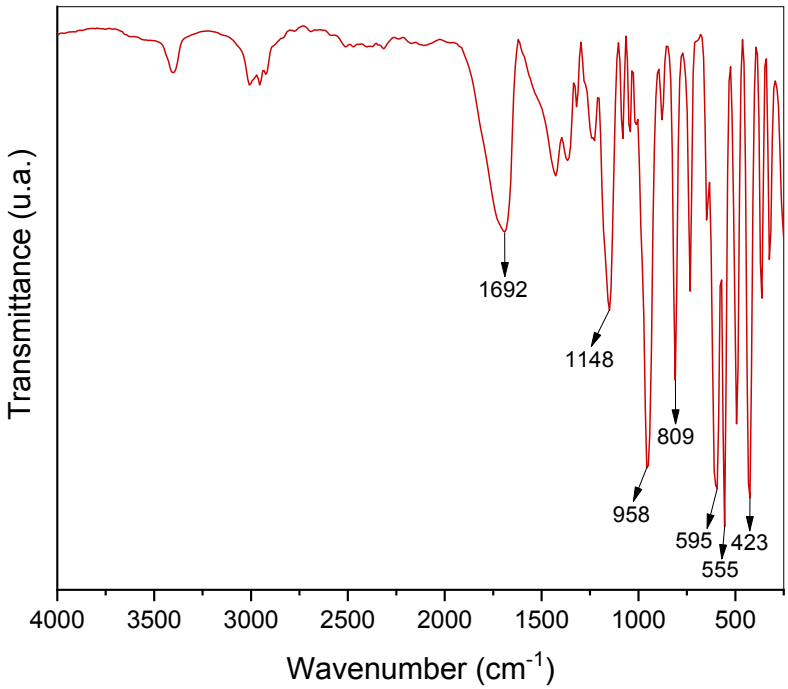

Figure S6. FT-IR Spectrum of P

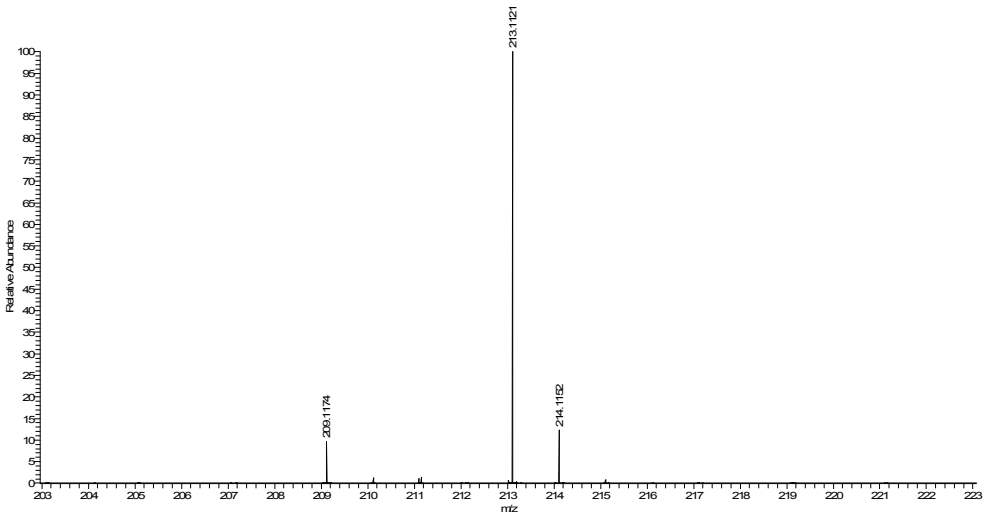

Figure S7. HRMS Spectrum of P

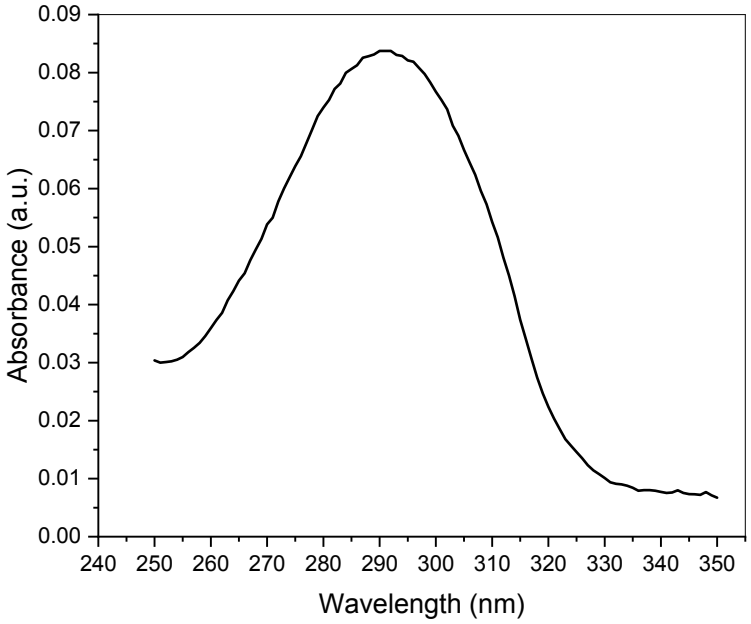

Figure S8. UV-Vis Spectrum of P

Step 2. Synthesis of Linker H_2L

In a 250 mL two- neck round bottom flask, the compound P(2.50 g, 0.012 mol) was dissolved in ethyl acetate (125 mL) and acetic acid (25 mL). The mixture was left under reflux and stirring for one hour until complete dissolution. After cooling down to room temperature, 4-hydrazinobenzoic acid (3.90 g, 0.026 mol) was added and then it was kept under reflux and stirring for 24 hours. A light pink product was filtered, washed with water and ethyl acetate three times each and dried in a vacuum oven at 60 °C for 12 hours.

Yield: 83%. **^{1}H NMR (**400 MHz, DMSO-d_6, 298K): δ/ppm= 13.02 (s, 2H, H_{32}), 8.03 (d, J_{HH}=8.60 Hz, 4H, $H_{24,26}$), 7.62 (d, J_{HH}=8.60 Hz, 4H, $H_{23,27}$), 3.54 (s, 2H, H_2), 2.29 (s, 6H, H_{12}),

2.07 (s, 6H, H_{13}). **^{13}C NMR {^{1}H}** (100 MHz, DMSO-d_6, 298K): δ/ppm= 166.74 (C_{31}), 148.14 (C_4), 143.19 (C_{16}), 136.19 (C_7), 130.30 ($C_{24,26}$), 128.43 (C_{25}), 123.21 ($C_{23,27}$), 116.63 (C_3), 17.59 (C_2), 12.14 (C_{13}), 11.21(C_{12}). **DEPT-135** (100 MHz, DMSO-d_6, 298 K): δ/ppm 130.75 ($C_{24,26}$), 123.65 ($C_{23,27}$), 18.03 (C_2), 12.58 (C_{13}), 11.65(C_{12}). **^{1}H,^{13}C-HSQC** (400 MHz/100 MHz, DMSO-d_6, 298 K): δ(^{1}H)/δ(^{13}C) = 8.03/130.31 ($H_{24,26}/C_{24,26}$), 7.62/123.22 ($H_{23,27}/C_{23,27}$), 3.54/17.60 (H_2/C_2), 2.29/11.18 (H_{12}/C_{12}), 2.07/12.12 (H_{13}/C_{13}). **^{1}H,^{13}C-HMBC** (400 MHz/100 MHz, DMSO-d_6, 298 K): δ(^{1}H)/δ(^{13}C)= 8.03/143.20 ($H_{24,26}/C_{16}$), 7.62/128.41 ($H_{23,27}/C_{25}$), 3,54/116.65, 136.18, 148.13 ($H_2/C_{3,7,4}$), 2.29/116.65, 136.18 ($H_{12}/C_{3,7}$), 2.07/116.65, 148.13 ($H_{13}/C_{3,4}$). **FT-IR (KBr):** ν/cm^{-1}= 3672.47 (w), 3402.43 (w), 2924.09 (w), 2522.89 (w), 2036.83 (w), 1705.07 (s), 1604.77 (s), 1512.19 (m), 1481.33 (w), 1427.32 (s), 1373.32 (s), 1273.02 (s), 1172.72 (m), 1103.28 (m), 1064.71 (w), 1018.41 (w), 902.69 (m), 864.11 (m), 810.10 (w), 771.53 (m), 694.37 (m), 570.93 (m), 540.07 (m), 493.78 (w), 408.91 (w), 339.47 (w) **HRMS(HESI):** m/z [M]$^{+}$ calculated for $C_{25}H_{24}N_4O_4$ (444.18), found 445.1868. **UV** (nm): 294.

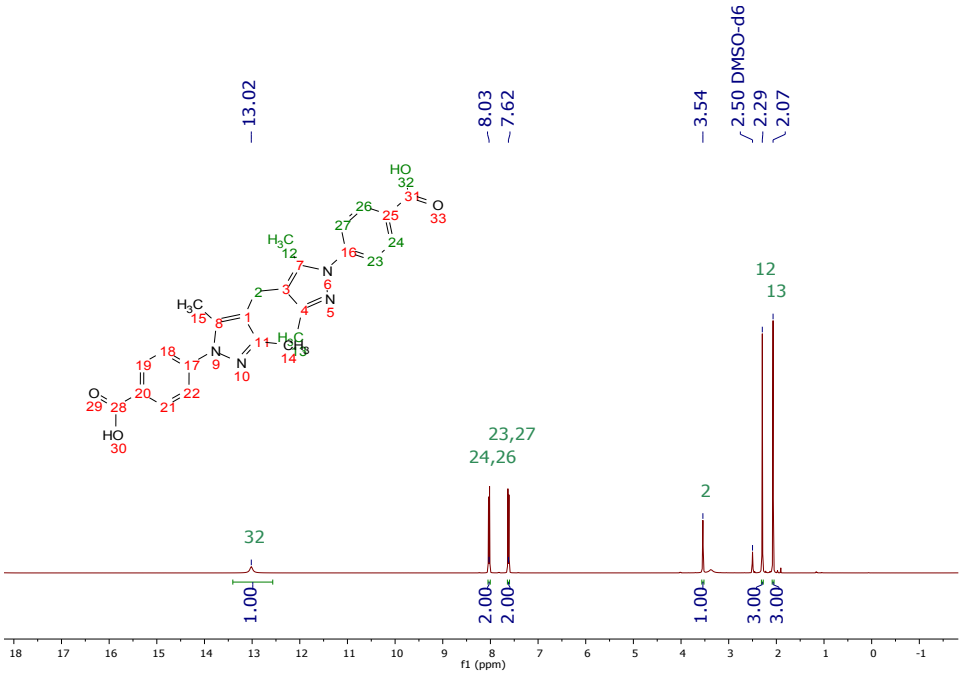

Figure S9. 400 MHz ^{1}H NMR spectrum of H_2L in DMSO-d_6.

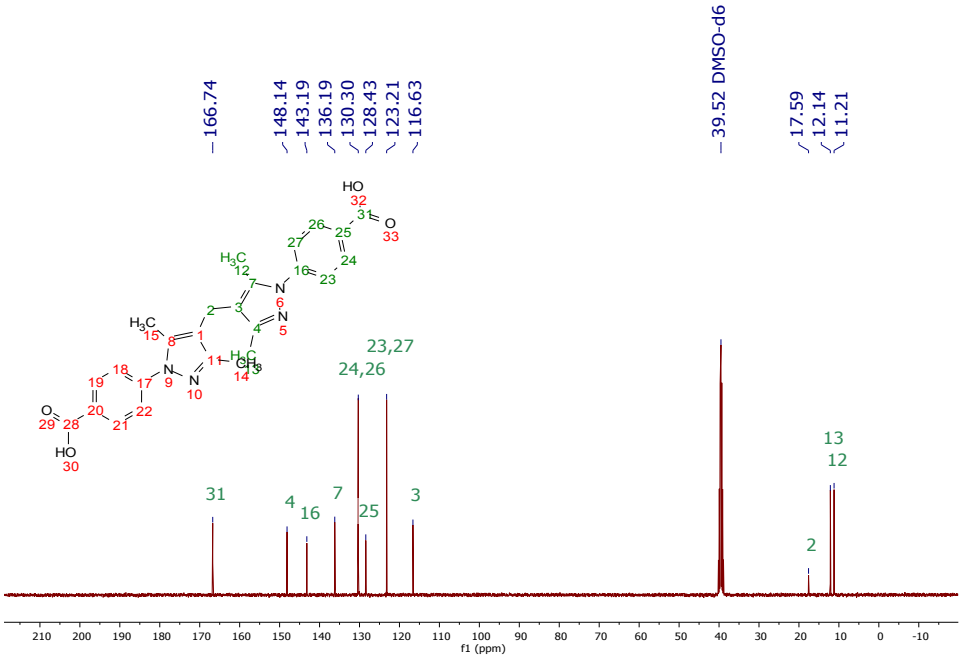

Figure S10. 400 MHz ^{13}C NMR spectrum of H_2L in DMSO-d_6.

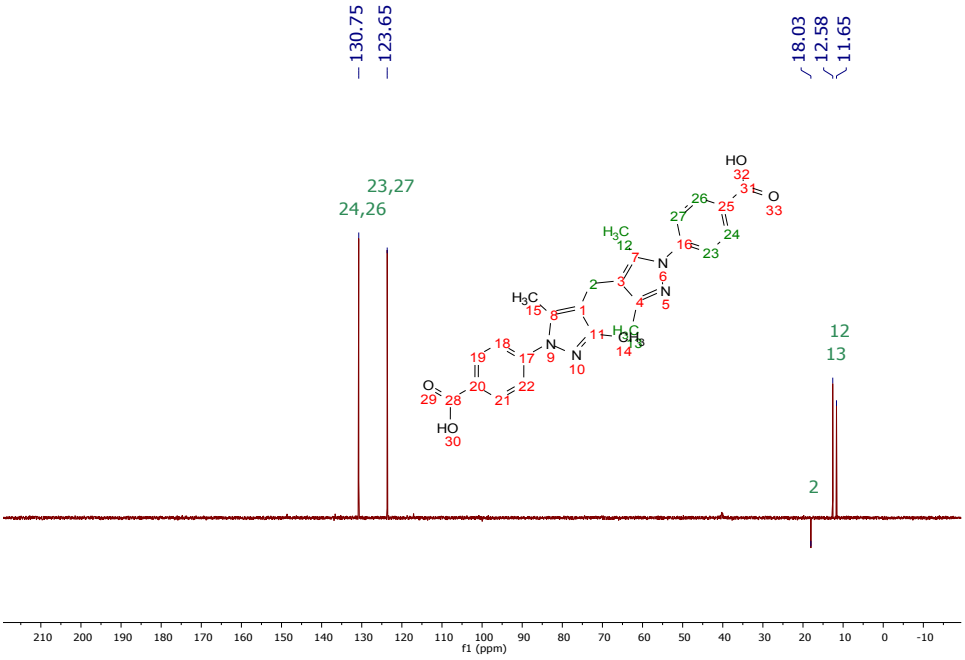

Figure S11. 400 MHz DEPT-135 NMR spectrum of H_2L in DMSO-d_6.

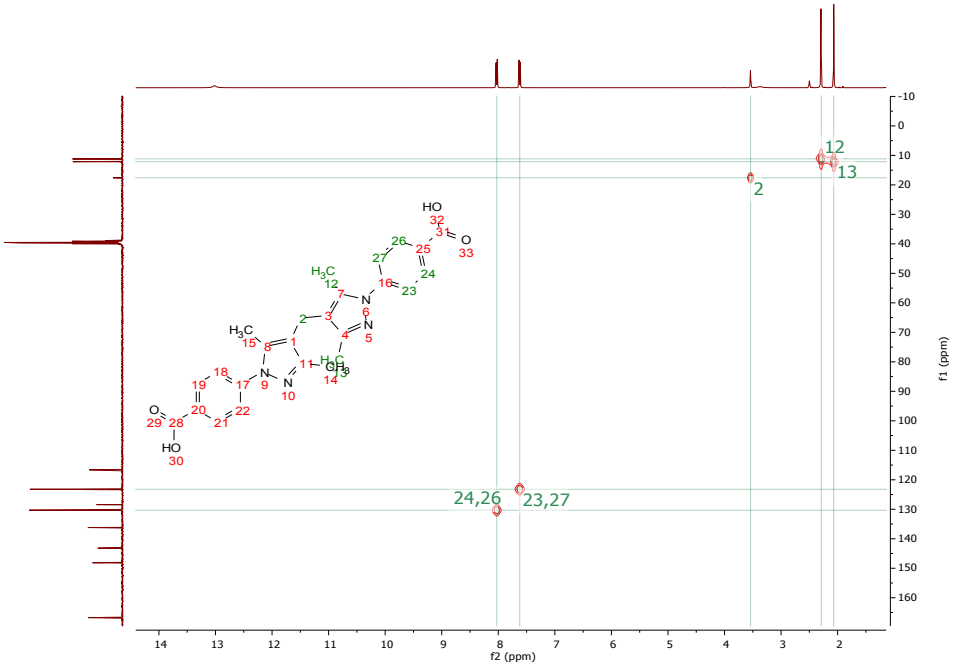

Figure S12. 400 MHz HSQC NMR spectrum of H_2L in DMSO-d_6.

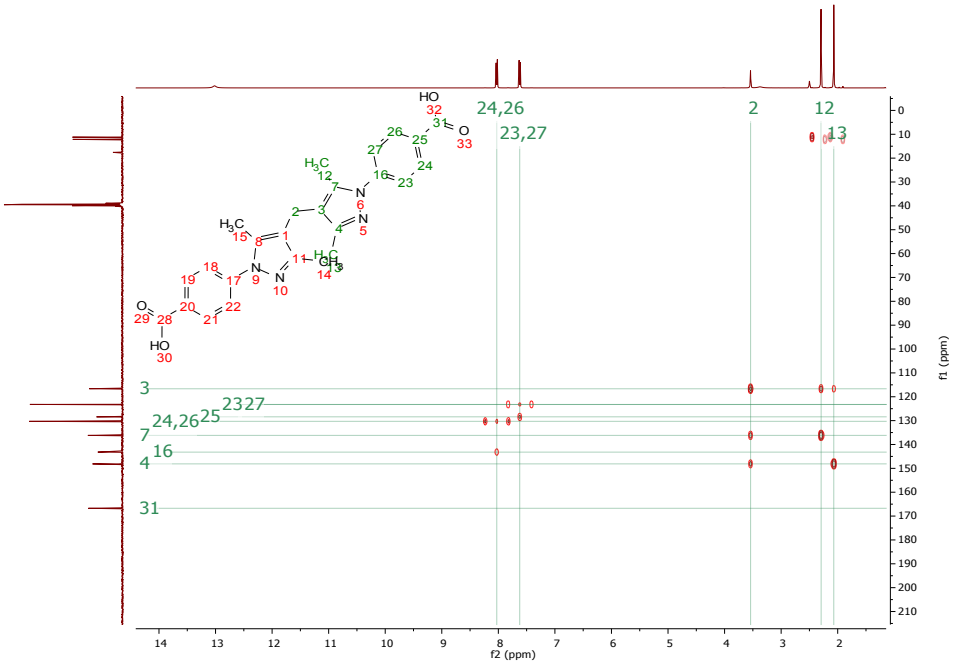

Figure S13. 400 MHz HMBC NMR spectrum of H_2L in DMSO-d_6.

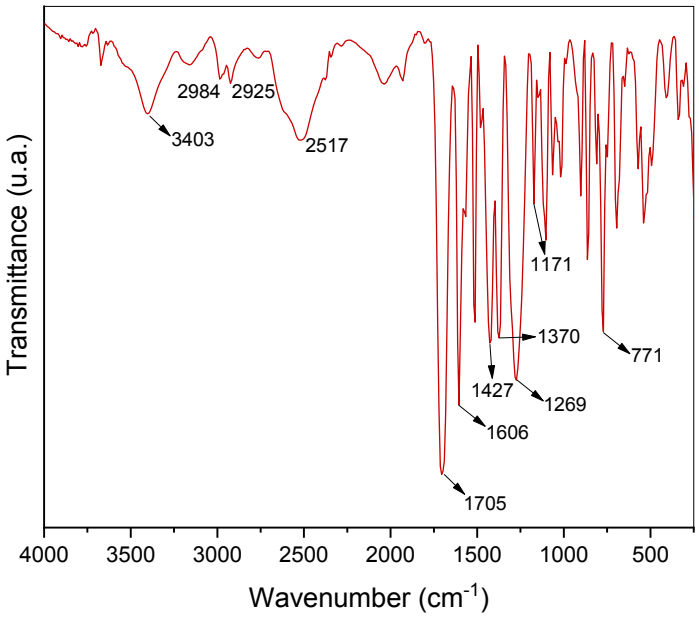

Figure S14. FT-IR Spectrum of H_2L

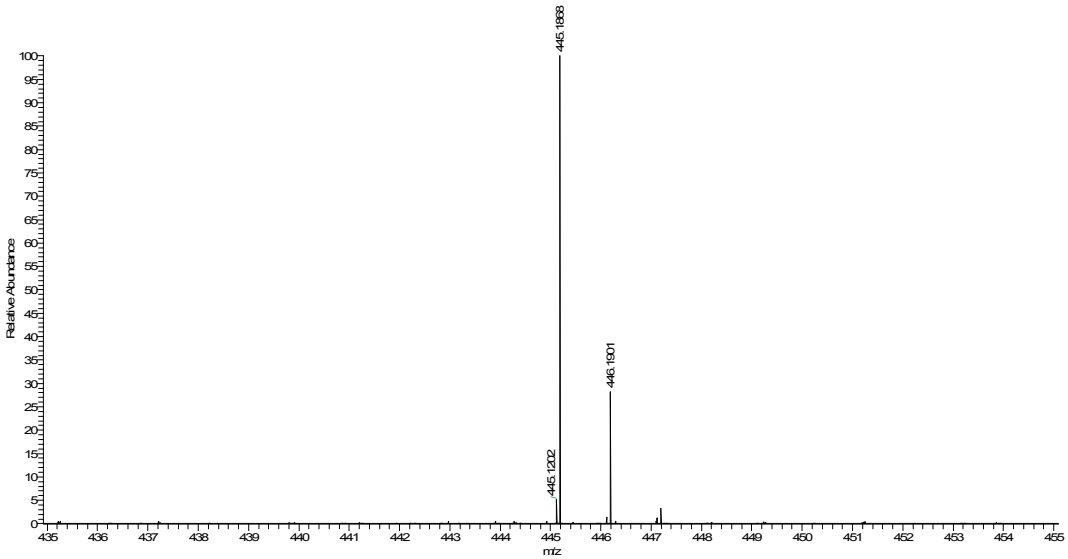

Figure S15. HRMS Spectrum of H_2L

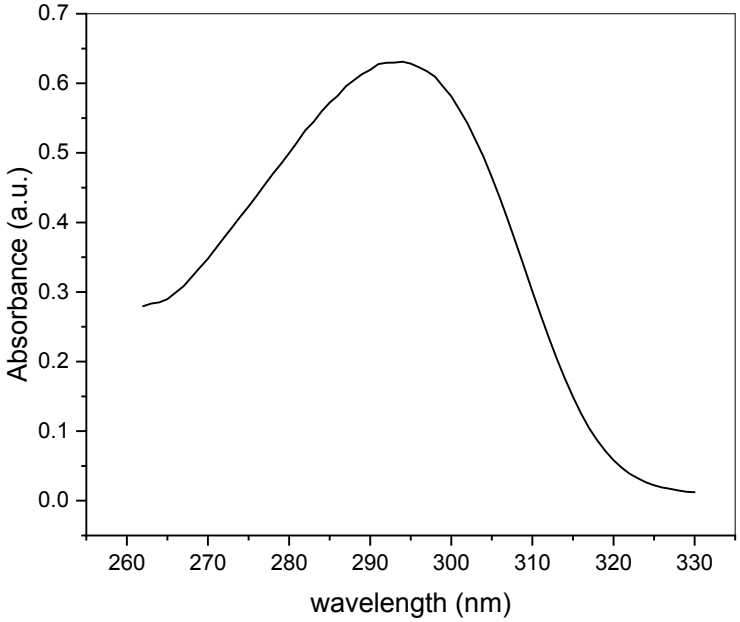

Figure S16. UV-Vis Spectrum of H_2L

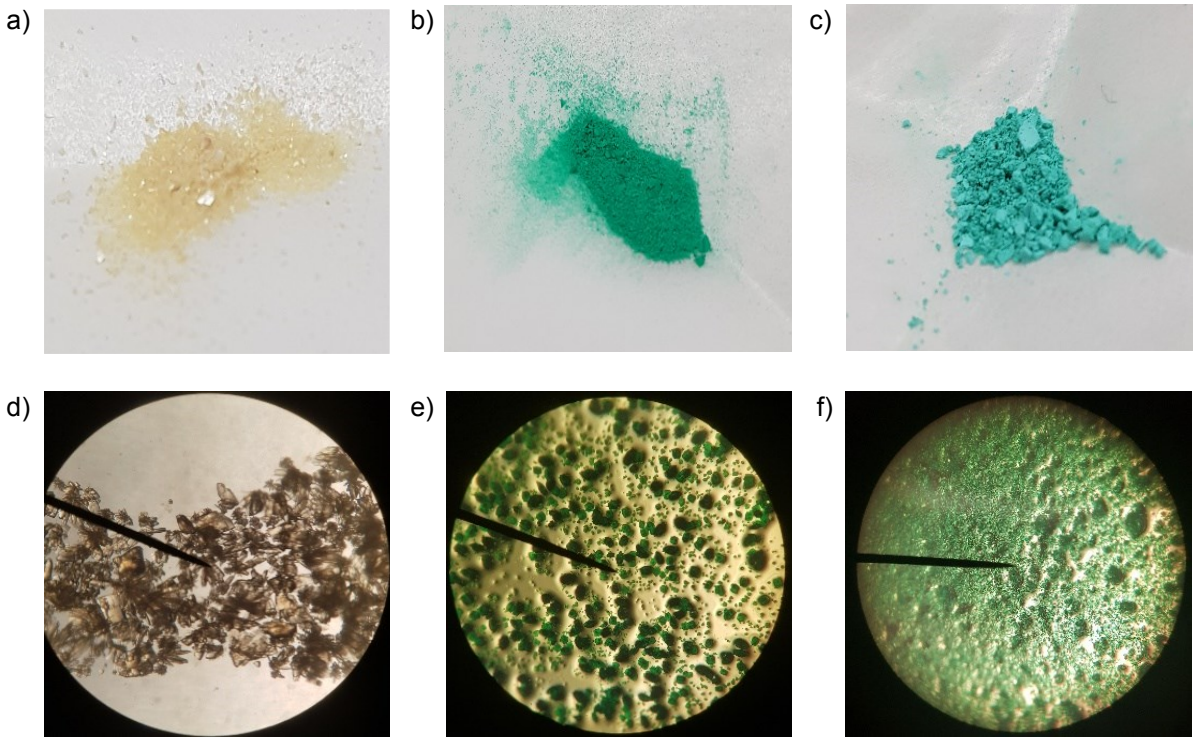

Figure S17. Physical aspect for a) [Zn^{II}(L)BPY], b) [Cu^{II}(L)BPY], and c) [Cu^{II}(L)DABCO] . Crystals images using an optical microscope for d) [Zn^{II}(L)BPY], e) [Cu^{II}(L)BPY], and f) [Cu^{II}(L)DABCO].

Identification code	[Zn^{II}(L)BPY]	[Cu^{II}(L)BPY]	[Cu^{II}(L)DABCO]
Empirical formula	$C_{36}H_{44}ZnN_7O_7$	$C_{30}H_{26}CuN_5O_4$	$C_{31}H_{36}CuN_6O_4$
Formula weight	752.189	584.10	620.20
Temperature/K	99.98(18)	100.02	100.01
Crystal system	monoclinic	monoclinic	monoclinic
Space group	C2/m	C2/m	$P2_1/n$
a/Å	18.3045(4)	18.1598(14)	9.3159(2)
b/Å	24.0896(6)	24.203(2)	26.0056(4)
c/Å	14.0301(3)	13.9450(11)	13.1078(2)
α3.9	90	90	90
β0 9	97.598(2)	97.387(3)	101.233(2)
γ7.3	90	90	90
Volume/$Å^3$	6132.2(2)	6078.4(8)	3114.73(10)
Z	8	8	4
ρ_{calc}g/cm^3	1.629	1.277	1.323
μ.mm^{-1}	0.870	0.759	1.353
F(000)	3164.1	2416.0	1300.0
Crystal size/mm^3	0.3 × 0.2 × 0.1	0.20×0.10×0.05	0.112 × 0.073 × 0.028
Radiation	MoKα (λ = 0.71073)	MoKα (λ = 0.71073)	CuKα (λ = 1.54184)
2Θ range for data collection/°	3.84 to 67.64	2.818 to 60.2	6.798 to 146.71°
Index ranges	-27 ≤ h ≤ 21, -33 ≤ k ≤ 36, -21 ≤ l ≤ 20	-25 ≤ h ≤ 25, -34 ≤ k ≤ 33, -19 ≤ l ≤ 19	-11 ≤ h ≤ 9, -31 ≤ k ≤ 31, -16 ≤ l ≤ 16
Reflections collected	43086	60389	21276
Independent reflections	10944 [R_{int} = 0.0256, R_{sigma} = 0.0278]	9118 [R_{int} = 0.0366, R_{sigma} = 0.0393]	6032 [R_{int} = 0.0488, R_{sigma} = 0.0444]
Data/restraints/parameters	10944/0/415	9118/75/398	6032/0/389
Goodness-of-fit on F^2	1.012	1.036	1.084
Final R indexes [I>=2eters	R_1 = 0.0466, wR_2 = 0.1267	R_1 = 0.0555, wR_2 = 0.1492	R1 = 0.0521, wR_2 = 0.1301
Final R indexes [all data]	R_1 = 0.0619, wR_2 = 0.1352	R_1 = 0.0842, wR_2 = 0.1641	R1 = 0.0614, wR_2 = 0.1376
Largest diff. peak/hole / e $Å^{-3}$	0.89/-0.76	0.95/-0.56	0.65/-0.67

Table S1. Crystal data and structure refinement for pillar-MOFs

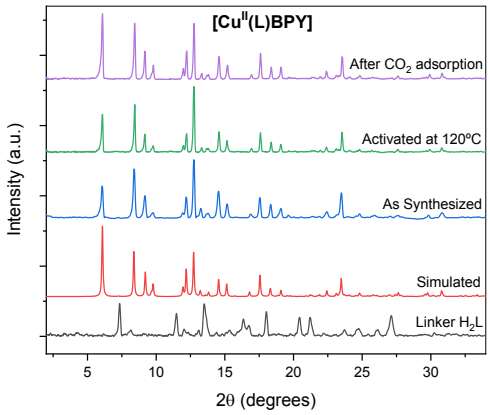

Figure S18. PXRD patterns for [Cu^{II}(L)BPY]. Linker H_2L (black); simulated (red); as-synthesized (blue); activated at 120ºC x 16h (green); and after CO_2 adsorption (purple).

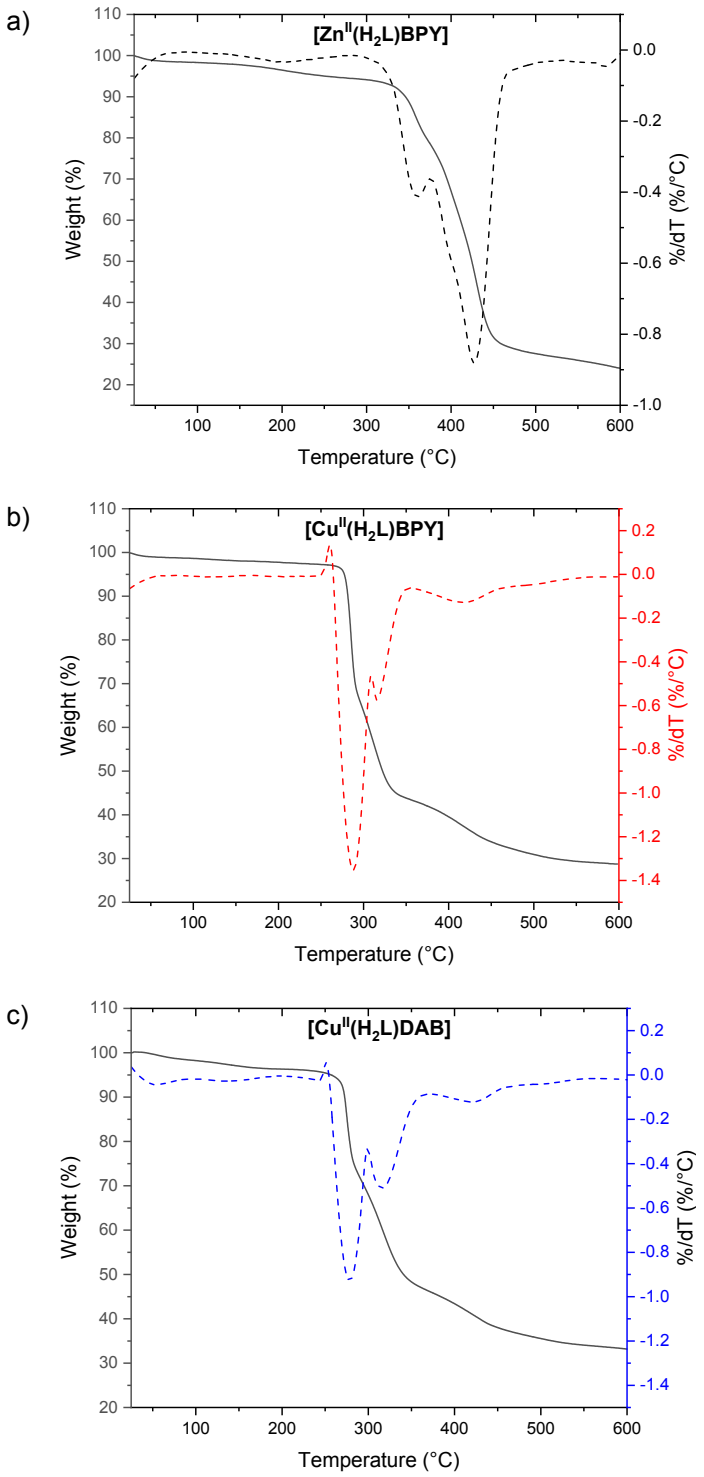

Figure S19. TGA profiles for a) [Zn^{II}(L)BPY], b) [Cu^{II}(L)BPY], and c) [Cu^{II}(L)DABCO]

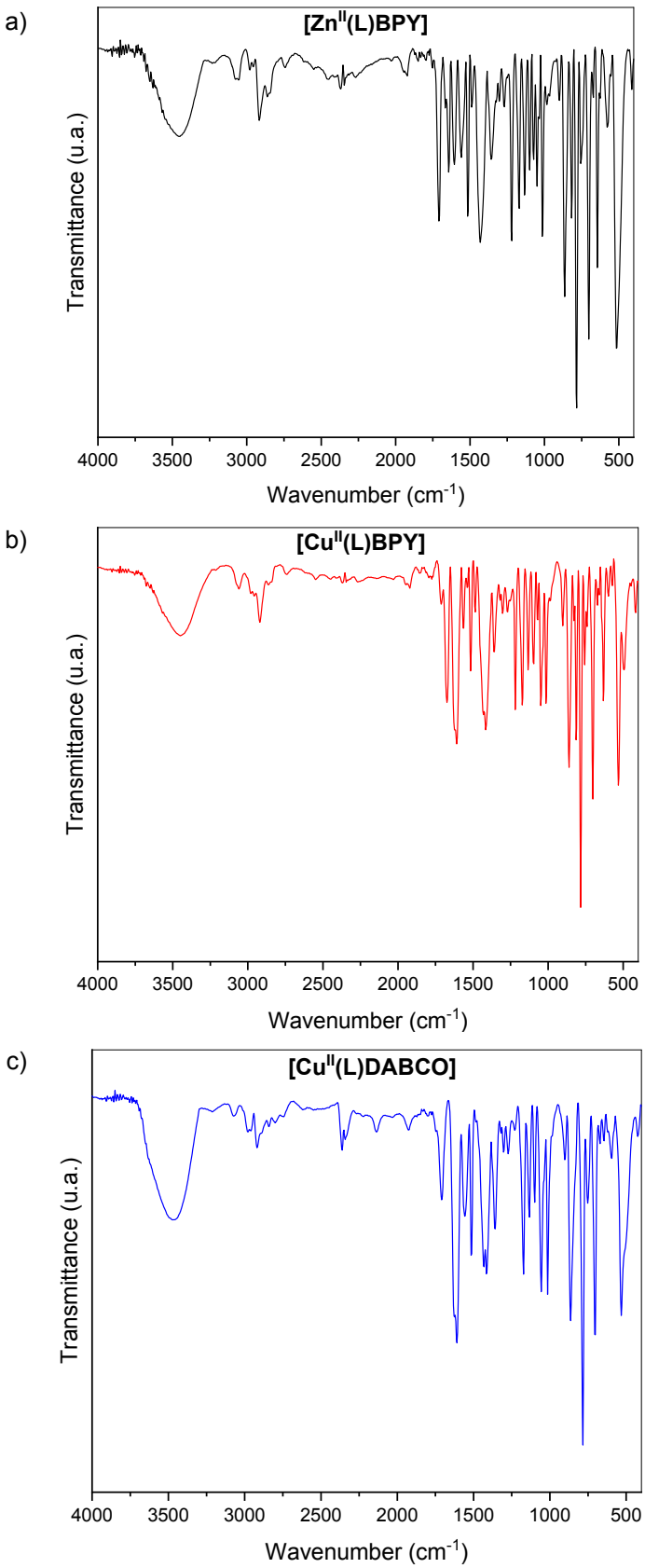

Figure S20. FT-IR spectra for a) [Zn^{II}(L)BPY], b) [Cu^{II}(L)BPY], and c) [Cu^{II}(L)DABCO]

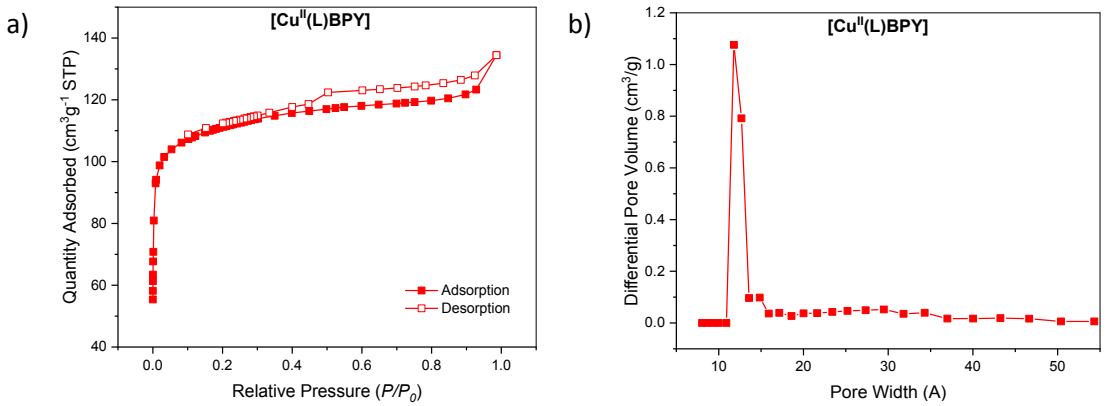

Figure S21. a) Nitrogen sorption isotherms at 77 K, and b) DFT calculated pore size distributions for [Cu^{II}(L)BPY]

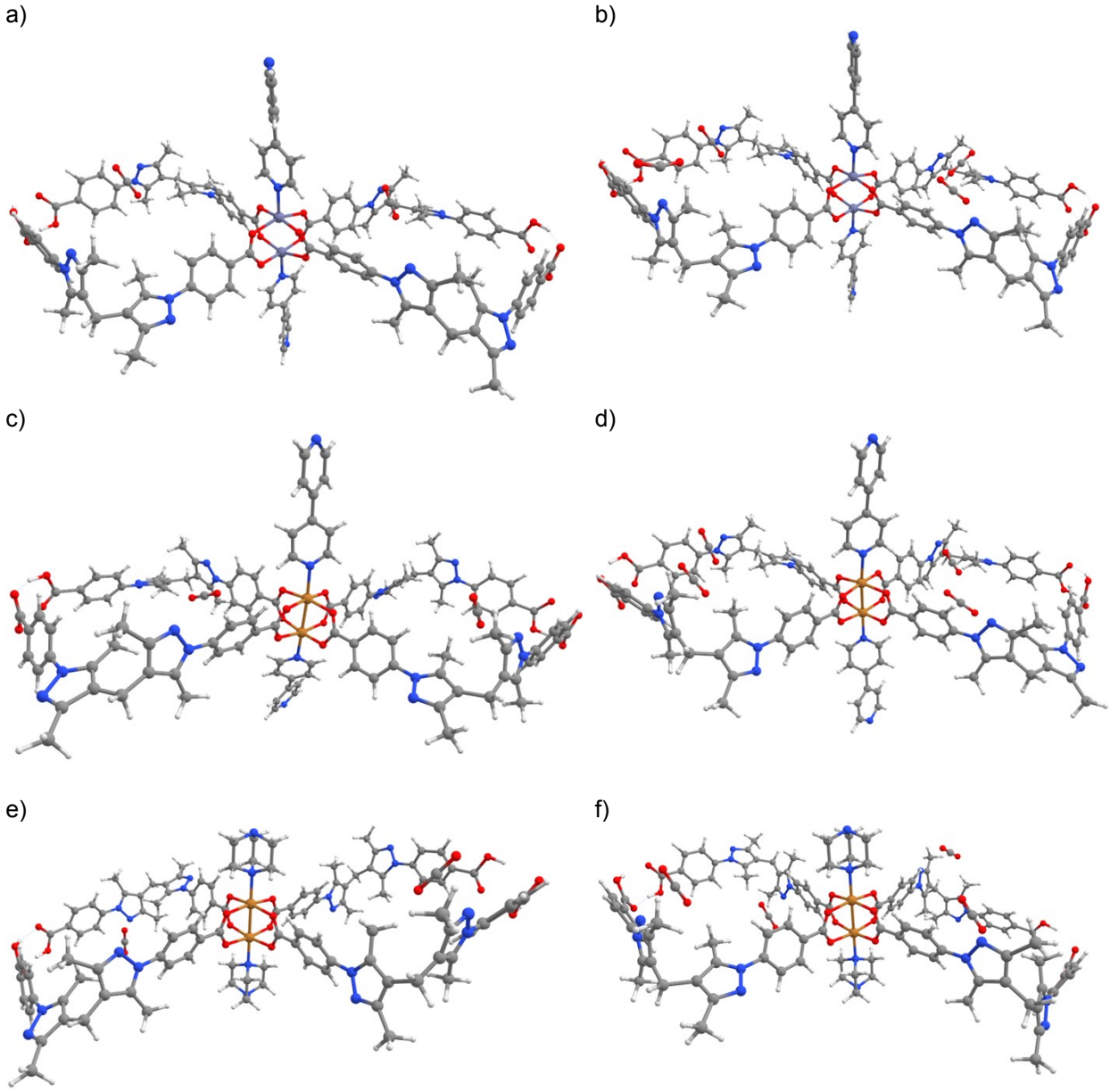

Figure S22. Studied MOFs and the adsorbed CO_2 molecules through the free nitrogen. [Zn^{II}(L)BPY] with a) 2 CO_2 molecules and b) 4 CO_2 molecules. [Cu^{II}(L)BPY] with c) 2 CO_2 molecules and d) 4 CO_2 molecules. [Cu^{II}(L)DABCO] with e)2 CO_2 molecules and f) 4 CO_2 molecules.

Table S2. Uptake of CO_2 at different temperatures for [Zn^{II}(L)BPY], [Cu^{II}(L)BPY], and [Cu^{II}(L)DABCO]

Temp	**[Zn^{II}(L)BPY]**				**[Cu^{II}(L)BPY]**				**[Cu^{II}(L)DABCO]**			
(K)	(cm^3/g)	(mg/g)	(mmol/g)	(wt%)	(cm^3/g)	(mg/g)	(mmol/g)	(wt%)	(cm^3/g)	(mg/g)	(mmol/g)	(wt%)
195	42.18	83.52	1.90	8.35	91.68	181.53	4.12	18.15	156.33	309.53	7.03	30.95
273	17.14	33.94	0.77	3.39	26.69	52.83	1.20	5.28	36.38	72.03	1.64	7.20
298	13.53	26.79	0.61	2.68	19.88	39.36	0.89	3.94	32.67	64.69	1.47	6.47

Table S3. Morokuma-Ziegler EDA in Kcal/mol for the structures optimized with CO_2 proximal to the free nitrogen.

		ΔE_{Pauli}	ΔE_{Elec}	ΔE_{Orb}	ΔE_{Dis}	ΔE_{Int}
[Zn^{II}(L)BPY]	2 CO_2	12.9	-7.9	-2.7	-10.8	-8.5
	4 CO_2	80.7	-42.7	-26.2	-22.2	-10.3
[Cu^{II}(L)BPY]	2 CO_2	14.1	-8.2	-3.9	-11.1	-9.1
	4 CO_2	26.9	-16.5	-6.7	-21.5	-17.8
[Cu^{II}(L)DABCO]	2 CO_2	14.0	-7.8	-6.3	-11.7	-11.8
	4 CO_2	21.4	-12.0	-7.4	-21.0	-18.9

Table S4. Elemental analysis of the MOFs

	Theoretical (%)	Experimental (%)
[Zn^{II}(L)BPY]	C: 61.4, H: 4.4, N: 11.9	C: 59.9, H: 4.1, N: 11.6
[Cu^{II}(L)BPY]	C: 61.6, H: 4.45, N: 11.9	C: 55.7, H: 3.96, N: 11.4
[Cu^{II}(L)DABCO]	C: 59.9, H: 5.8, N: 13.54	C: 59.89, H: 4.24, N: 11.63

References

(1) Tomar, K.; Verma, A.; Bharadwaj, P. K. Exploiting Dimensional Variability in Cu Paddle-Wheel Secondary Building Unit Based Mixed Valence Cu(II)/Cu(I) Frameworks from a Bispyrazole Ligand by Solvent/PH Variation. *Cryst. Growth Des.* **2018**, *18* (4), 2397–2404. https://doi.org/10.1021/acs.cgd.8b00002.

(2) Burton, S.; Fronczek, F. R.; Maverick, A. W. 3,5-Diacetyl-Heptane-2,6-Dione. *Acta Crystallogr. Sect. E Struct. Reports Online* **2007**, *63* (7), 0–5. https://doi.org/10.1107/S1600536807026323.